SCIENTIFIC REPORTS

OPEN

High performance surface-modified TiO_2/silicone nanocomposite

Pei Huang[1], Han-Qiao Shi[2,3], Hong-Mei Xiao[3], Yuan-Qing Li[1], Ning Hu[1] & Shao-Yun Fu[1,3]

Received: 30 September 2016
Accepted: 25 May 2017
Published online: 20 July 2017

The mismatch of refractive index (RI) between light emitting diode (LED) chips and packaging resins severely lowers the lighting emitting efficacy of LED. The RI can be enhanced by the introduction of high RI nanoparticles but meanwhile it is a great challenge to maintain the high transparency for resins due to the agglomeration of nanoparticles. In this work, a facile strategy is proposed to fabricate silicone nanocomposites with a high transparency (>88%, less than 2% decrease relative to pure silicone resin), largely enhanced RI (an increase from 1.42 to 1.60) and improved thermal stability (73 °C increase in weight loss of 50%). Specifically, the ultra-fine monodispersed TiO_2/silicone composites are prepared by direct solvent mixing of 1 wt% surface modified TiO_2 nanoparticles (S-TiO_2) into the silicone resin, in which S-TiO_2 are prepared by direct introduction of titanate coupling agent in the process of TiO_2 growth to induce the formation of protective layer on the surfaces of TiO_2 nanoparticles. This methodology demonstrated is simple, cost-effective and versatile for the massive fabrication of highly transparent LED packaging materials with greatly enhanced refractive index and meanwhile enhanced thermal stability.

Light emitting diodes (LEDs) have drawn considerable interests in the last several decades due to their high lighting efficiency and lighting wavelength tunability[1–4]. In a typical LED device, lighting chip and packaging material are the main components which determine the light emitting efficacy. Concerning the long-term service of LEDs, transmittance, refractive index (RI) and thermal stability are the key criteria required for packaging materials. Silicone resin is endorsed as the first choice over other types of materials (such as epoxy resin, polymethyl methacrylate, etc.) due to its high thermal stability and facile fabrication process[5–7]. However, the RI mismatch between the lighting chip and silicone resin leads to severe light reflection at the interface of LED chip and silicone resin, and thus greatly lowers the light emitting efficacy[8]. Great efforts have been made to increase the RI of silicone resin by introduction of functionalized atoms and side chains, or bottom-up design of polymer structure[9–14]. Currently, commercial silicone resins with relatively high RI are available[15], whereas their very high prices and complicated processing procedures hinder their wide applications as LED packaging materials.

According to the Maxwell–Garnett effective medium theory[16], the incorporation of inorganic filler with high RI can increase the RI of the polymer matrix[8]. TiO_2 with a high RI (n = 2.45 and 2.7 for anatase and rutile phase, respectively) and a very low absorption coefficient in the visible range is highly attractive as a filler for the fabrication of high RI packaging materials[17,18]. However, the poor dispersion of nanoparticles in the polymer matrix is a great challenge due to their high surface energy. Although various methods have been developed to improve the dispersion of TiO_2 nanoparticles in silicone resin, likewise, surface modification of TiO_2 nanoparticle in the process of sol-gel[19–21], modification of silicone resin and etc.[22,23]. However, these approaches usually involve toxic agents and complicated processing procedures of synthesis, purification, mixing of TiO_2 nanoparticles[24], and so on. Therefore, a simple yet environmental-friendly approach is strongly required to fabricate highly transparent silicone nanocomposites with high RI and high thermal stability.

Recently, a facile approach to prepare size-controllable ZnO nanoparticle has been reported by the introduction of coupling agent into precursor[24,25]. In this work, a similar strategy has been applied to synthesize surface modified ultra-fine TiO_2 (S-TiO_2) nanoparticles through the introduction of titanate coupling agent in the process of TiO_2 nanoparticle growth. The protective layer formed on the surfaces of TiO_2 nanoparticles can effectively prevent the growth of TiO_2 nanoparticles and significantly improve the compatibility between TiO_2 nanoparticles and the silicone resin. In principle, the introduction of inorganic TiO_2 can enhance the thermal

[1]College of Aerospace Engineering, Chongqing University, Chongqing, 400044, China. [2]Aerospace Research Institute of Materials & Processing Technology, Beijing, 100076, China. [3]Technical Institute of Physics and Chemistry, Chinese Academy of Sciences, Beijing, 100190, China. Pei Huang and Han-Qiao Shi contributed equally to this work. Correspondence and requests for materials should be addressed to Y.-Q.L. (email: yqli@cqu.edu.cn) or S.-Y.F. (email: syfu@cqu.edu.cn)

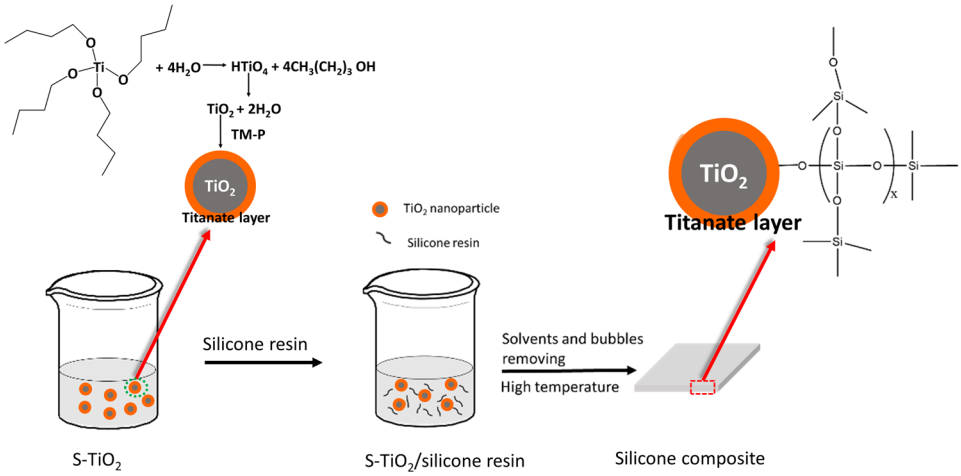

Figure 1. Illustration of the fabrication of S-TiO_2/silicone nanocomposites.

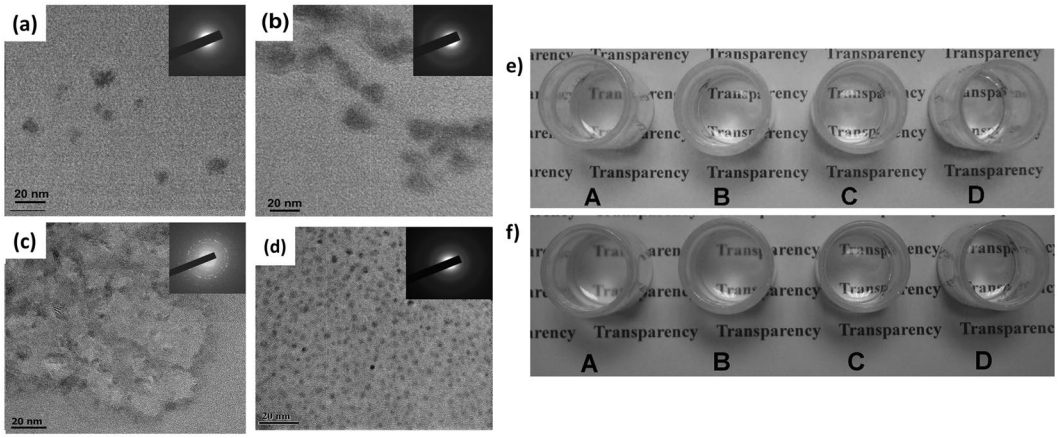

Figure 2. TEM images of (**a**) TiO_2-1, (**b**) TiO_2-2, (**c**) TiO_2-3 and (**d**) S-TiO_2; solubility of (**e**) S-TiO_2 and (**f**) silicone resin in (A) acetone, (B) petroleum ether, (C) cyclohexane and (D) acetic ether.

stability of polymers. Thus, a highly transparent TiO_2/silicone nanocomposite with a high RI and high thermal stability can be obtained by directly mixing the ultra-fine S-TiO_2 nanoparticles with the silicone resin. To evaluate their potential as LED packaging material, the transmittance, RI and thermal stability of the as-prepared silicone nanocomposite are examined. As a control, several types of TiO_2 nanoparticles without the introduction of coupling agent and the corresponding composites are prepared and compared with the surface modified S-TiO_2 case.

Results and Discussions

Synthesis of S-TiO_2. Figure 1 shows the general steps to fabricate S-TiO_2/silicone nanocomposites. First, the TiO_2 nanoparticles synthesized via sol-gel approach were introduced into silicone resin/acetic ether solution under ultrasonic treatment, forming a uniform suspension. Subsequently, the resulting suspension was subjected to a vacuum chamber to remove acetic ether and bubbles. Finally, the transparent nanocomposites were prepared by curing the resin at 100 °C. The only difference of the preparation procedure between S-TiO_2/silicone nanocomposite and un-treated TiO_2/silicone nanocomposite is the introduction of titanate coupling agent, which endows TiO_2 nanoparticles with protective layers on their surface.

The morphology of the as-prepared TiO_2 materials was characterized by TEM. As shown in Fig. 2, the TiO_2-1 has a diameter of approximately 5 nm. Increasing the reaction time from 48 h to 72 h leads to an increase of the diameter of TiO_2-2 nanoparticles from ca. 10 to ca. 15 nm, accompanying with TiO_2 aggregation. TiO_2-3 obtained by drying TiO_2-2 at 120 °C for 24 h shows a significant increase in the diameter of particles up to the scale of micrometer. By contrast, S-TiO_2 nanoparticles with a diameter of 3–4 nm are mono-dispersed in the composite. The afore-mentioned results are supported by the BET measurement. As shown in Table S1, specific surface areas of 35.8, 17.6, 2.84, and 75.6 m^2/g are achieved for TiO_2-1, TiO_2-2, TiO_2-3 and S-TiO_2, respectively, which agrees well with the result for the diameter of TiO_2 nanoparticles. X-ray diffraction patterns (top insets of Fig. 2a–d) indicate that the crystallinity of TiO_2 increases with the increases of reaction time and temperature. Additional evidence on the chemical structure of the TiO_2 particles was provided by EDS analysis. C originated from titanate coupling agent is observed in S-TiO_2 while no trace of C is found in TiO_2-1, TiO_2-2 and TiO_2-3 (Table S1), indicating formation of protective layers on the

	TiO_2-1	TiO_2-2	TiO_2-3	S-TiO_2
Transparency*	X	X	X	O

Table 1. Dispersibility of various TiO_2 particles in acetic ether. *Note: Turbid: X, Transparent: O.

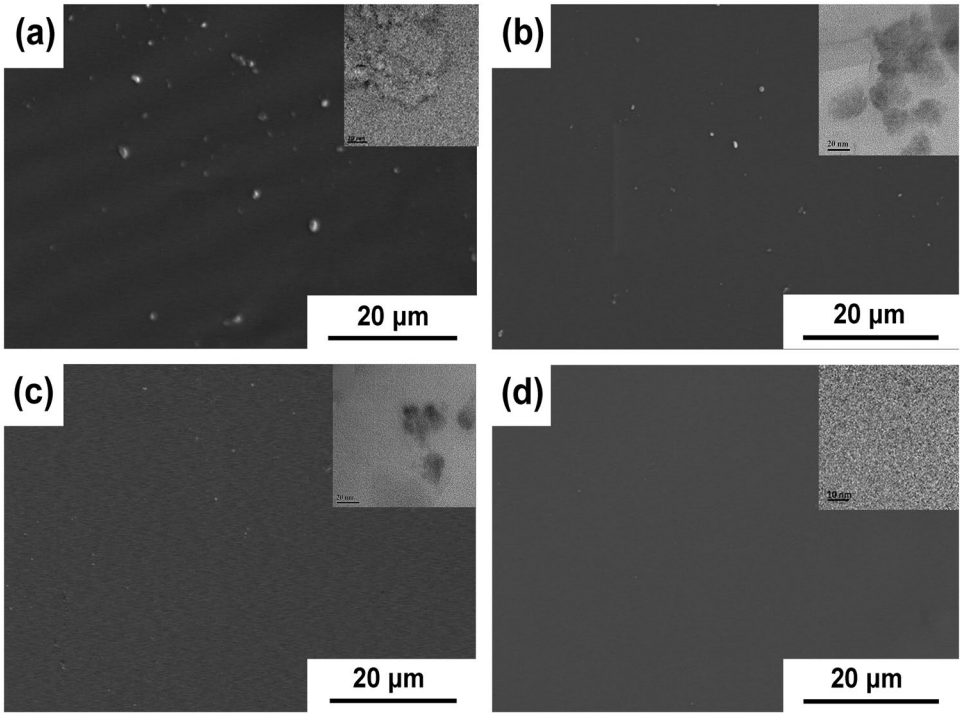

Figure 3. SEM images of the cross sections of silicone nanocomposites with 1 wt% (**a**) TiO_2-3, (**b**) TiO_2-2, (**c**) TiO_2-1, and (**d**) S-TiO_2 (top inset: TEM image of the corresponding TiO_2/silicone nanocomposite).

surfaces of S-TiO_2. Due to the formation of protective layers on their surfaces during the growth of TiO_2 nanoparticles, the increase of the TiO_2 diameter is declined and stopped until the formation of intact layers on their surfaces.

Dispersibility of TiO_2. To achieve a homogenous dispersion of TiO_2 in silicone resin, co-solvent is needed to dilute silicone resin due to the poor solubility of silicone resin in ethanol. As shown in Fig. 2e and f, the suspensions of S-TiO_2 and silicone resin formed in acetic ether both are transparent, while their suspensions formed in other solvents including acetone, petroleum ether and cyclohexane are turbid. In addition, acetic ether featured by low toxicity and low boiling point is a good candidate for the massive fabrication of TiO_2/silicone nanocomposite. The dispersity of TiO_2-1, TiO_2-2 and TiO_2-3 in acetic ether was also investigated via the same strategy. As presented in Table 1, all of the suspensions of TiO_2-1, TiO_2-2 and TiO_2-3 formed in acetic ether are turbid, indicating that the dispersibility of S-TiO_2 in acetic ether is much better than that of TiO_2 without surface modification. In addition, to reveal the effectiveness of various surface modifiers in improving the dispersibility of TiO_2, the transparency of their suspensions in acetic ether was further studied. As presented in Table S2, all of the suspensions of TiO_2 modified by oxalic acid, citric acid, KH-550 and KH-560 are turbid, indicating that titanate coupling agent is the most effective in improving the dispersibility of TiO_2 in acetic ether.

Transmittance of TiO_2/silicone nanocomposites. The cross sections of silicone nanocomposites of various TiO_2 nanoparticles were observed with SEM. As shown in Fig. 3a–c, aggregates sized ca. 150 nm, 30 nm and 10 nm are observed in the nanocomposites incorporated with TiO_2-1, TiO_2-2, and TiO_2-3, respectively, suggesting the poor dispersion of TiO_2-1, TiO_2-2 and TiO_2-3 in the silicone resin. In comparison, no visible aggregates appear in the S-TiO_2/silicone nanocomposite. S-TiO_2 nanoparticles are mono-dispersed in the silicone resin with a diameter around 3–4 nm (see the top inset of Fig. 3d). The narrow size distribution and excellent dispersion of S-TiO_2 in the silicone resin are attributed to the titanate coupling agent layers formed on the surfaces of TiO_2 nanoparticles, endorsing the excellent compatibility between TiO_2 nanoparticles and silicone resin, and thus eliminating the aggregation of TiO_2 nanoparticle in both acetic ether and silicone resin.

The following equation gives the light intensity of a spherical particulate composite[26,27]:

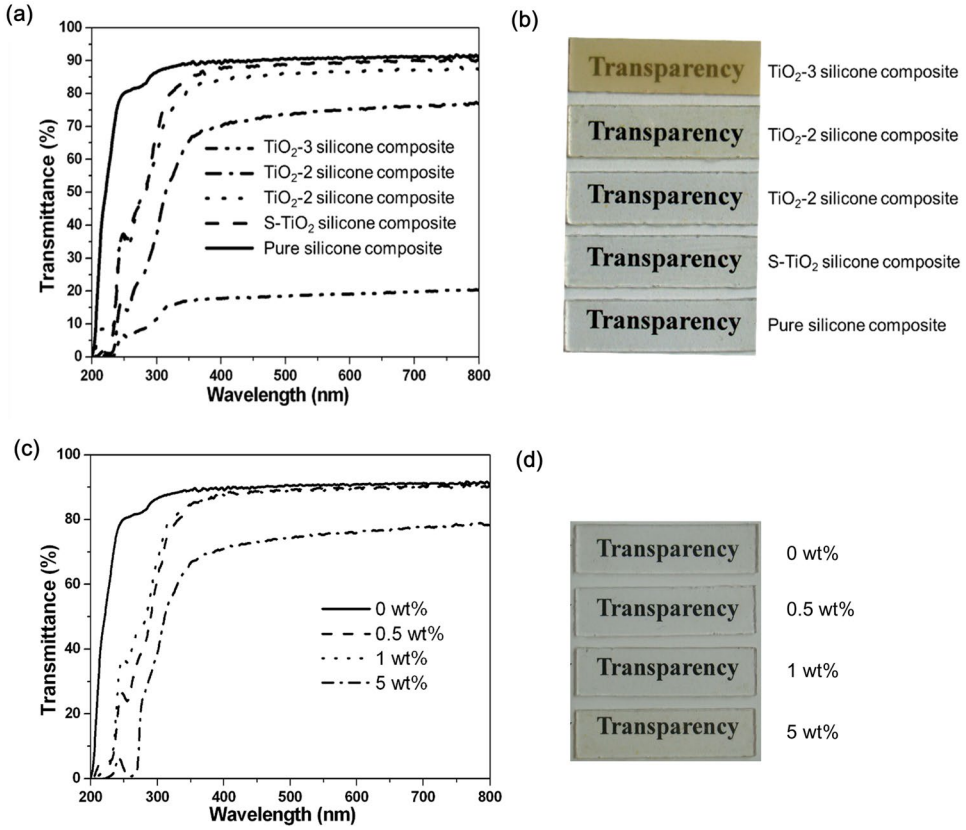

Figure 4. (**a**) Transmittance and (**b**) photograph of the silicone nanocomposite with 1 wt% TiO_2-3, TiO_2-2, TiO_2-1 and S-TiO_2, and pure silicone as the control; (**c**) transmittance and (**d**) corresponding photograph of titanate S-TiO_2/silicone nanocomposites with varied S-TiO_2 mass fractions.

$$\frac{I}{I_0} = \exp\left\{\left[-\frac{32V_p x\pi^4 r^3}{\lambda^4}\left(\frac{(n_p/n_m)^2 - 1}{(n_p/n_m)^2 + 2}\right)^2\right]\right\} \quad (1)$$

where r, n_p and V_p are the radius, RI and volume fraction of spherical particles, respectively. n_m is the RI of matrix, λ is light wavelength, and x is the thickness of the composite. As revealed in Equation 1, the diameter of nano-filler significantly affects the transmittance of the composite. Therefore, to maintain the high transparency of the composite, the ultra-fine nano-fillers with mono-dispersion are strongly required. Meanwhile, the transmittance of a composite is highly related to the thickness of composites, it is quite difficult to achieve a high transparency for bulk materials than thin films. To our best knowledge, all of the transparent composites with enhanced RI reported previously are thin films with a thickness of 10^{-8} to 10^{-4} m, whereas bulk transparent nanocomposites with a thickness of 10^{-3} to 10^{-2} m are rarely reported[27–30]. The thickness of the resin layer as encapsulating material surely has some effect on the lighting efficiency of LED. In this study, the thickness of the as-prepared silicone composite is ca. 1 mm (namely ca. 10^{-3} m), close to that of realistic packaging materials for LEDs. This could give us practical evaluation of the current protocol on the performance of the as-prepared silicone composite. The high specific surface area of nanoparticles would lead to irreversible aggregation[32,33]. Aggregated nanoparticles usually have much larger sizes than individual nanoparticles, and thus would have an adverse effect on the transparency and lighting efficiency of LED. In this work, S-TiO_2 nanoparticles are mono-dispersed in the silicone resin, and thus the resultant composite as encapsulating material has a high transparency (Fig. 4). As a result, the introduction of S-TiO_2 would have no adverse effect on the efficiency of LED.

Figure 4a shows the transmittance of the pure silicone resin and silicone nanocomposites with 1 wt% TiO_2. Compared with the pure silicone resin, only 2% decrease in transmittance is achieved in the S-TiO_2/silicone nanocomposite. As the TiO_2 particle size increases, the transparency of silicone nanocomposite decreases. Figure 4b visually demonstrates the transparency of the corresponding silicone nanocomposites. The transparency of TiO_2-1/silicone nanocomposite and TiO_2-2/silicone nanocomposite is approximately 83% and 75%, respectively. Further increase in the particle size of TiO_2 results in an opaque silicone nanocomposite with 20% of transmittance in the visible light range. This change obeys Equation 1.

The effect of S-TiO_2 filler content on the transmittance is shown in Fig. 4c. With the addition of 0.5 and 1.0 wt% S-TiO_2, the transmittance of silicone nanocomposite is close to that of pure silicone resin, and the average decrease of the transmittance in the visible range of 400–800 nm is less than 2%. As revealed in Fig. 4d, no

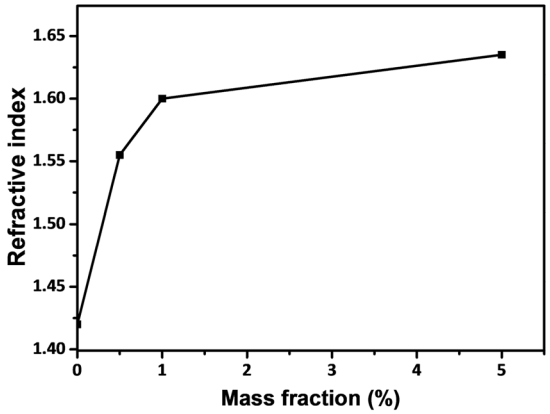

Figure 5. RI of S-TiO_2/silicone nanocomposites with different mass fractions.

visible transparency difference is seen with naked eyes between the pure silicone resin and the nanocomposites filled with 0.5 and 1.0 wt% of S-TiO_2. Even increasing the content of S-TiO_2 up to 5.0 wt%, the transmittance in the visible range still maintains at a high level of approximately 70%, indicating that the surface modification of TiO_2 with titanate coupling agent is very effective in fabricating highly transparent TiO_2/polymer nanocomposite.

RI of TiO_2/silicone nanocomposites. The lighting efficiency of LED can be determined by the difference of refractive index between lighting chips and packaging materials as indicated by Equation 2 [31]:

$$\eta_{encapsulated} = \left(\frac{1 - \cos\left(\arcsin\frac{n_{pm}}{n_{chip}}\right)}{1 - \cos\left(\arcsin\frac{1}{n_{chip}}\right)} \right) \eta_{unencapsulated} \quad (2)$$

where $\eta_{encapsulated}$ and $\eta_{unencapsulated}$ are the lighting efficiency of encapsulated and un-encapsulated LED chip, respectively; n_{pm} and n_{chip} are the refractive index of packaging materials and LED chip, respectively. It is understandable from Equation 2 that as the RI of the packaging material increases, the lighting efficiency first increases quasi-linearly, then sub-linearly, and finally reaches a saturation. Since the RI of conventional lighting chip material is 2.5~3.0, the packaging material with a higher RI will lead to a higher lighting efficiency of LED. In this work, the introduction of fine TiO_2 particles with a high RI brings about a high RI of the composite as encapsulating material, aiming at increasing the lighting efficiency of LED.

The RI measured for the silicone nanocomposite with 1 wt% S-TiO_2, TiO_2-1, TiO_2-2, and TiO_2-3 is 1.596, 1.596, 1.602, and 1.642, respectively. The RI of silicone nanocomposite filled with TiO_2-3 is somewhat higher than other nanocomposites, due to the crystallinity of TiO_2-3 formed with longer aging time is better than that of S-TiO_2, TiO_2-1, and TiO_2-2. Figure 5 shows the RI of S-TiO_2/silicone nanocomposites as a function of S-TiO_2 mass fraction. As the S-TiO_2 loading increases from 0 to 0.5 and 1 wt%, the RI of silicone resin is dramatically increased from 1.42 to 1.56 and 1.596, achieving the improvement of 9.8% and 12.3%, respectively. In comparison with other researches, the current strategy shows higher improvements in RI. For instance, the incorporation of 1% of silane modified TiO_2 and oleic acid capped TiO_2 in to silicone resin increases the RI of silicone composite from 1.51 to 1.56 and 1.575, respectively[32,33]. As the content of S-TiO_2 increases further, the increasing rate of the RI is declined. Less than 2% of increase in RI is achieved as the content of S-TiO_2 increases further to 5 wt%, indicating that the effectiveness of RI enhancement at a higher filler content is limited. In principle, the porosity if any would reduce the RI of the composite since the air has a RI of unity. In the current work, the porosity measured on the surfaces of TiO_2 particles was around 3%. On the other hand, silicone resin might penetrate into the porosity. As a result, the effect of the porosity on the RI could be neglected. Therefore, the RI of the composite was determined mainly by TiO_2 particles and enhanced by the incorporation of TiO_2 particles as confirmed by Fig. 5.

Thermal stability of TiO_2/silicone nanocomposite. Figure 6 shows the TGA curves of the pure silicone resin and the silicone nanocomposites with various S-TiO_2 loadings. Although the starting decomposition temperature is almost the same for the pure silicone resin and the silicone nanocomposites, the incorporation of TiO_2 nanoparticles decreases the decomposition speed of the silicone nanocomposite. Taking the example of the weight loss of 50%, the temperature of the silicone nanocomposites with 0%, 1% and 5% S-TiO_2 is 532, 605 and 632 °C, respectively; namely, the temperature corresponding to the weight loss of 50% has been increased by 73 and 100 °C, respectively. The "cross-link density" of the nanocomposites is increased with the incorporation of TiO_2 nanoparticles, which leads to the enhancement of their thermal stability with a decreased decomposition rate[34].

Conclusions

In summary, a facile approach to produce highly transparent TiO_2/silicone nanocomposite with a high RI and a high thermal stability has been demonstrated by the incorporation of S-TiO_2 nanoparticles treated by titanate coupling agent into diluted silicone resin via simple solvent mixing. The titanate coupling agent layers formed on the

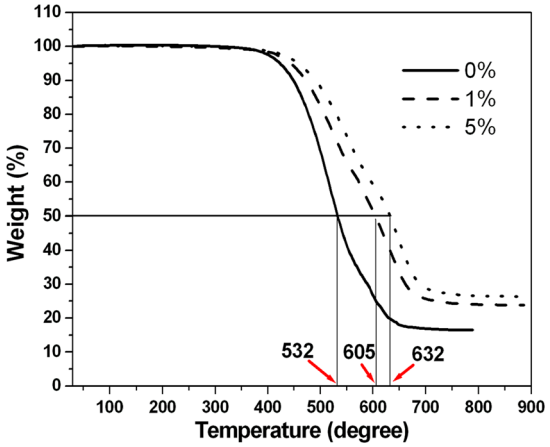

Figure 6. TGA curves of pure silence resin and S-TiO_2/silicone nanocomposites with 1 wt% and 5 wt% S-TiO_2.

surfaces of ultra-fine 3–4 nm TiO_2 nanoparticles endorses the excellent dispersion of S-TiO_2 nanoparticles in the silicone resin and an excellent compatibility between the TiO_2 nanoparticles and the silicone resin. Consequently, with the addition of 1 wt% S-TiO_2, the as-prepared silicone nanocomposite shows an enhanced RI from 1.42 to ca. 1.60 (13% enhancement), a high transmittance of 88% in the entire visible light range for 1 mm thick samples and meanwhile an enhanced thermal stability. The current strategy is cost-effective, environmental-friendly, and easy-processing, which has a great potential to be widely used in producing transparent packaging materials with the greatly enhanced RI and meanwhile a high thermal stability.

Materials and Methods

Materials. Tetrabutyl titanate ($C_{16}H_{36}TiO_4$) was purchased from Beijing Xingjin Chemical Reagent Company. Absolute ethanol, acetic ether, acetone, petroleum ether, and cyclohexane were supplied by Beijing Chemistry Reagent Company and used as received. Titanate coupling agent (TM-P) was bought from JiangSu YiZheng TianYang Chemical Plant. Silicon resin (KMT-1252) with two parts A and B was purchased from Beijing KMT Technology Co., Ltd.

Synthesis of S-TiO_2 nanoparticles. S-TiO_2 nanoparticles were prepared with a typical sol-gel procedure. First, 0.01 M tetrabutyl titanate was added to 50 mL ethanol, then the solution was stirred for 15 min to ensure complete dissolution of tetrabutyl titanate. Afterwards, 0.12 mL TM-P was introduced into the suspension and stirred for another 15 min. Subsequently, 1 mL distilled water was added to the suspension obtained and kept stirring for 48 h at 40 °C.

In parallel, TiO_2 nanoparticles with different sizes were synthesized using the similar protocol in the absence of the titanate coupling agent TM-P. The samples react for 48 h and 72 h, denoted as TiO_2-1 and TiO_2-2, respectively. TiO_2-3 was prepared by vacuum drying of TiO_2-2 at the temperature of 120 °C for 24 h.

Fabrication of TiO_2/silicone nanocomposites. In a typical fabrication procedure, 10 g silicon resin with the mass ratio of 10:1 for Part A and Part B was dissolved in 20 mL acetic ether by ultrasonic treatment until a transparent solution was obtained. Then, 0.11 g TiO_2 particles (TiO_2-1, TiO_2-2, TiO_2-3 or S-TiO_2) were homogenously mixed with silicone resin/acetic ether solution by ultrasonic treatment. The bubbles and acetic ether were removed by vacuum pump. Finally, the resultant suspension was casted into a stainless steel mould and then transferred into an oven at 100 °C for 2 h. The thickness of as-prepared silicone composites is approximately 1 mm.

Characterizations. The transmittance of the nanocomposite was obtained from a Hitachi U-3900. The RI was measured on an Abbe Refractometer (WAY-2S) in ambient atmosphere. Transmission electron microscopy (TEM) images and electronic diffraction were taken on a JEM-2100F instrument (operated at 200 kV). Scanning electron microscopy (SEM) images and energy dispersive spectroscopy (EDS) were collected on a Hitachi S-4300. The Brunauer–Emmett–Teller (BET) specific surface areas were calculated using adsorption data in P/P0 = 0.05–0.3 (six points collected). The weight loss analysis of the samples was conducted on a Netzsch STA 409 PC/PG at the rate of 10 °C/min under nitrogen atmosphere. Fourier transform infrared (FTIR) spectra were recorded using a Varian 3100 FT-IR spectrometer with 2 cm^{-1} resolution and accumulation of 24 scans.

References

1. Ellingson, R. J. *et al.* Highly efficient multiple exciton generation in colloidal PbSe and PbS quantum dots. *Nano Letters* **5**, 865–871 (2005).
2. Narukawa, Y., Ichikawa, M., Sanga, D., Sano, M. & Mukai, T. White light emitting diodes with super-high luminous efficacy. *J. Phys. D: Appl. Phys.* **43**, 354002 (2010).
3. Yang, Y. *et al.* High-performance multiple-donor bulk heterojunction solar cells. *Nat. Photon* **9**, 190–198 (2015).
4. Lee, S., Hong, J.-Y. & Jang, J. Multifunctional graphene sheets embedded in silicone encapsulant for superior performance of light-emitting diodes. *ACS Nano* **7**, 5784–5790 (2013).
5. Arik, M., Setlur, A., Weaver, S., Haitko, D. & Petroski, J. Chip to system levels thermal needs and alternative thermal technologies for high brightness LEDS. *J. Electron. Packag.* **129**, 328–338 (2007).
6. Maehara, T. *et al.* Synthesis and polymerization of novel epoxy compounds having an adamantane ring and evaluation of their heat resistance and transparency. *J.Appl. Polym. Sci.* **112**, 496–504 (2009).

7. Gao, N., Liu, W., Yan, Z. & Wang, Z. Synthesis and properties of transparent cycloaliphatic epoxy–silicone resins for opto-electronic devices packaging. *Opt.Mater.* **35**, 567–575 (2013).
8. Li, Y.-Q., Fu, S.-Y., Yang, Y. & Mai, Y.-W. Facile synthesis of highly transparent polymer nanocomposites by introduction of core–shell structured nanoparticles. *Chem. Mater.* **20**, 2637–2643 (2008).
9. Yang, C.-J. & Jenekhe, S. A. Group contribution to molar refraction and refractive index of conjugated polymers. *Chem. Mater.* **7**, 1276–1285 (1995).
10. Rogers, H. *et al*. Highly amorphous, birefringent, para-linked aromatic polyamides. *Macromolecules* **18**, 1058–1068 (1985).
11. Yang, C. J. & Jenekhe, S. A. Effects of structure on refractive index of conjugated polyimines. *Chem. Mater.* **6**, 196–203 (1994).
12. Koynov, K. *et al*. Molecular weight dependence of chain orientation and optical constants of thin films of the conjugated polymer MEH-PPV. *Macromolecules* **39**, 8692–8698 (2006).
13. Hsu, C.-Y., Han, W.-G., Chiang, S.-J., Su, W.-C. & Liu, Y.-L. Multi-functional branched polysiloxanes polymers for high refractive index and flame retardant LED encapsulants. *RSC Adv* **6**, 4377–4381 (2016).
14. Tapaswi, P. K., Choi, M.-C., Jeong, K.-M., Ando, S. & Ha, C.-S. Transparent aromatic polyimides derived from thiophenyl-substituted benzidines with high refractive index and small birefringence. *Macromolecules* **48**, 3462–3474 (2015).
15. Bahadur, M., Norris, A. W., Zarisfi, A., Alger, J. S. & Windiate, C. C. Silicone materials for LED packaging. In *Sixth International Conference on Solid State Lighting*, 63370F (2006)
16. Aspnes, D. E. Local-field effects and effective-medium theory: A microscopic perspective. *Amer. J. Phys.* **50**, 704–709 (1982).
17. Nakayama, N. & Hayashi, T. Preparation and characterization of TiO2–ZrO2 and thiol-acrylate resin nanocomposites with high refractive index via UV-induced crosslinking polymerization. *Compos. Part A* **38**, 1996–2004 (2007).
18. Tao, P. *et al*. TiO_2 nanocomposites with high refractive index and transparency. *J. Mater. Chem.* **21**, 18623–18629 (2011).
19. De, S. & De, G. *In situ* generation of Au nanoparticles in UV-curable refractive index controlled SiO_2—TiO_2—PEO hybrid Films. *The Journal of Physical Chemistry C* **112**, 10378–10384 (2008).
20. Yang, S., Kim, J.-S., Jin, J., Kwak, S.-Y. & Bae, B.-S. Cycloaliphatic epoxy oligosiloxane-derived hybrid materials for a high-refractive index LED encapsulant. *J.Appl. Polym. Sci.* **122**, 2478–2485 (2011).
21. Guan, C., Lü, C.-L., Liu, Y.-F. & Yang, B. Preparation and characterization of high refractive index thin films of TiO2/epoxy resin nanocomposites. *J. Appl. Polym. Sci.* **102**, 1631–1636 (2006).
22. Yang, X. *et al*. Preparation and performance of high refractive index silicone resin-type materials for the packaging of light-emitting diodes. *J. Appl.Polym. Sci.* **127**, 1717–1724 (2013).
23. Tuan, C. C. et al. Ultra-high refractive index LED encapsulant. In 2014 IEEE 64th Electronic Components and Technology Conference (ECTC), 447–451 (2014).
24. Huang, P. *et al*. Greatly decreased redshift and largely enhanced refractive index of mono-dispersed ZnO-QD/silicone nanocomposites. *J.Mater. Chem. C* **4**, 8663–8669 (2016).
25. Shi, H.-Q. *et al*. Synthesis of silane surface modified ZnO quantum dots with ultrastable, strong and tunable luminescence. *Chem. Commun.* **47**, 11921–11923 (2011).
26. Novak, B. M. Hybrid nanocomposite materials—between inorganic glasses and organic polymers. *Adv. Mater.* **5**, 422–433 (1993).
27. Althues, H., Henle, J. & Kaskel, S. Functional inorganic nanofillers for transparent polymers. *Chem. Soc. Rev.* **36**, 1454–1465 (2007).
28. Chau, J. L. H. *et al*. Transparent high refractive index nanocomposite thin films. *Mater. Lett.* **61**, 2908–2910 (2007).
29. Nakayama, N. & Hayashi, T. Preparation and characterization of TiO_2 and polymer nanocomposite films with high refractive index. *J. Appl. Polym. Sci.* **105**, 3662–3672 (2007).
30. Elim, H. I. *et al*. Refractive index control and rayleigh scattering properties of transparent TiO_2 nanohybrid polymer. *J. Phys. Chem. B* **113**, 10143–10148 (2009).
31. Ma, M. *et al*. Effects of the refractive index of the encapsulant on the light-extraction efficiency of light-emitting diodes. *Opt. Express* **19**, A1135–A1140 (2011).
32. Liu, Y. *et al*. High refractive index and transparent nanocomposites as encapsulant for high brightness LED packaging. *IEEE Trans. Compon., Packag. Manufact. Technol.* **4**, 1125–1130 (2014).
33. Cho, E.-C. *et al*. The optoelectronic properties and applications of solution-processable titanium oxide nanoparticles. *Org. Electronics* **18**, 126–134 (2015).
34. Liufu, S.-C., Xiao, H.-N. & Li, Y.-P. Thermal analysis and degradation mechanism of polyacrylate/ZnO nanocomposites. *Polym. Degrad. Stab.* **87**, 103–110 (2005).

Acknowledgements

This work is financially supported by National Natural Science Foundation of China (Nos 51573200, 51373187, 11372312 and 11572321) and the starting funding of Chongqing University (Nos 0903005203352 and 0241001104417).

Author Contributions

S.F. and Y.L. conceived the project. P.H. and H.S. performed the research. S.F., Y.L., H.X., N.H., P.H. and H.S. discussed the results and the experimental implementations. The manuscript was written through contributions of all authors. All authors have given approval to the final version of the manuscript.

Additional Information

Supplementary information accompanies this paper at doi:10.1038/s41598-017-05166-7

Competing Interests: The authors declare that they have no competing interests.

Publisher's note: Springer Nature remains neutral with regard to jurisdictional claims in published maps and institutional affiliations.